ACS APPLIED MATERIALS & INTERFACES

RESEARCH ARTICLE

www.acsami.org

Carbonaceous Materials Passivation on Amine Functionalized Magnetic Nanoparticles and Its Application for Metal Affinity Isolation of Recombinant Protein

Iryanti F. Nata, Nermeen S. El-Safory, and Cheng-Kang Lee*

Department of Chemical Engineering, National Taiwan University of Science and Technology, 43 Keelung Rd Sec. 4, Taipei 106, Taiwan

Supporting Information

ABSTRACT: Magnetic nanoparticles (MNPs) with an amine functionalized surface (MH) were passivated with carbonaceous materials (MH@C) by carbonization of glucose under hydrothermal reaction conditions. The carboxylate groups in carbonaceous shell could be enriched to 0.285 mmol/g when acrylic acid was added as a functional monomer in the carbonization reaction (MH@C−Ac). The carbonaceous shell not only protected the magnetic core from acidic erosion but also showed a high adsorption capacity toward Ni^{2+} ion. The Ni^{2+} ion complexed on MH@C and MH@C−Ac could specifically isolate 6×His tagged recombinant proteins from crude bacterial extracts via metal affinity interaction. The superparamagnetic property facilitates the easy retrieval of the carbonaceous material passivated MNPs from the viscous proteins solutions. Recombinant green fluorescence protein (GFP) and hyaluronic acid (HA) lyase of 9.4 mg and 2.3 mg could be isolated by 1 g of MH@C−Ac−Ni, respectively.

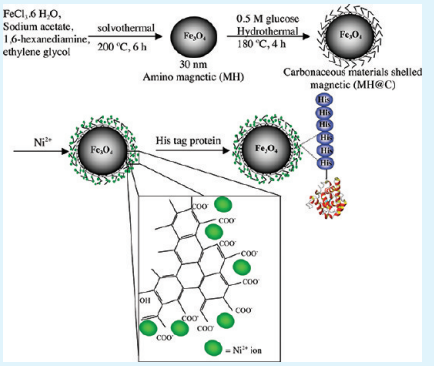

KEYWORDS: hydrothermal carbonization, magnetic carbonaceous nanoparticle, ion complexed, 6×His tagged protein, metal affinity interaction, protein isolation

1. INTRODUCTION

Magnetic particles with nanometer size have been a subject of great scientific and industrial interest because of their interesting electrical, magnetic, and chemical properties which cannot be achieved by their bulk counterparts. Magnetic nanoparticles (MNPs) have been widely applied in biotechnology, such as enzyme immobilization,[1] protein separation,[2−6] and nucleic acid separation.[7] Most of the magnetic particle supports synthesized for biological separation usually have a core−shell structure. The key element of shell structure has greatly attracted attention in recent years. Polysaccharides such as dextran[8] and chitosan[9] as well as inorganic silica[10,11] are commonly employed as a protective shell on MNPs so that the stable colloidal MNPs could be obtained. The protective coating not only can stabilize the nanoparticle but also can facilitate surface modification for its specific applications.

Glucose and other carbohydrates when treated under hydrothermal condition are known to form carbonaceous materials featuring a hydrophilic surface with mostly carboxyl and carbonyl functionalities. By hydrothermal carbonization of glucose, encapsulation of magnetic FeNi nanoparticles[12] and generation of a one-dimensional nanostructured carbon hybrid with Fe_3O_4 have been reported.[13] It has also been demonstrated that an amine-functionalized surface will promote the preferential deposition of carbonaceous materials on the surface during hydrothermal carbonization of glucose.[12] Therefore, we have prepared magnetic carbonaceous spheres based on one-pot hydrothermal carbonization of glucose with amine functionalized magnetic nanoparticles for heavy metal ions removal.[14] The magnetic carbonaceous particles demonstrated not only a good heavy metal ion adsorption capacity but also a low-pH resistant property.

In recent times, there has been a considerable interest in developing methods to capture target proteins directly from the crude extracts of recombinant microorganisms. The magnetic particle immobilized with various ligands such as metal chelating groups,[15−17] oligonucleotide,[18] and ion exchange[19] have been studied to achieve this goal. Due to the advances of genetic engineering techniques, most of the desired recombinant proteins can be produced with a 6×His tag in either the N- or C-terminal to facilitate their recovery via immobilized metal-ion affinity adsorption. The transition metal ions such as Ni^{2+} or Co^{2+} ion are most often immobilized as affinity metal ligands to specifically capture the 6×His tagged proteins. Since the carbonaceous particles generated from hydrothermal carbonization of glucose have demonstrated a high metal ion adsorption capability[14,20−22] due to its rich surface of carboxylate groups, in this work, carbonaceous material was passivated on surface amine functionalized MNPs (MH@C) to adsorb Ni^{2+} ion. The Ni^{2+} ion complexed magnetic nanoparticle was used as a magnetically retrievable metal ion affinity adsorbent for 6×His tagged protein isolation. The MNPs was surface functionalized with primary

Received: April 14, 2011
Accepted: August 10, 2011
Published: August 10, 2011

amine during its preparation in a mild solvothermal reaction. The size, morphology, thermal stability, functional groups, surface charge, and Ni^{2+} adsorption onto MH@C were characterized. Recombinant green fluorescent protein (GFP)[2,23−25] and hyaluronic acid (HA) lyase[26−31] with a 6×His tag fused on their structure have effectively been purified by immobilized metal affinity chromatography. Therefore, the 6×His tagged GFP and HA lyase were employed as model proteins to study the performance of the Ni^{2+} ion loaded MH@C for direct isolation from a crude protein extract.

2. EXPERIMENTAL SECTION

2.1. Materials. All ingredients of culture media were obtained from ACROS. All other chemicals were analytical grade and used without further purification.

2.2. Synthesis of Magnetic Nanoparticles. Surface amine-functionalized MNPs were synthesized according to the method described previously.[32] Briefly, anhydrous sodium acetate (1.6 g) and $FeCl_3 \cdot 6H_2O$ (0.8 g) were dissolved in ethylene glycol (24 mL) with vigorous stirring at 50 °C to give an orange solution. When 1,6-hexanediamine (HMDA) (7 mL) was added, the solution turned dark orange. Then, the solution was transferred into a Teflon container and sealed in a stainless steel autoclave. The autoclave was heated at 198 °C for 6 h in an oven. After cooling to room temperature, clear supernatant with black precipitate was obtained. The precipitate was collected by employing a magnet and washed with deionized (DI) water (250 mL) followed by 70% ethanol, each for 3 times. The obtained magnetic precipitate was designated as MH and kept in DI water for future use.

2.3. Passivation MNPs with Carbonaceous Materials. The as-prepared magnetic nanoparticle MH of 0.3 g (dry weight) was dispersed in 0.5 M glucose solution (15 mL) by sonication bath for 10 min. The well-suspended MH solution was transferred to a Teflon container sealed by a stainless steel autoclave and heated at 180 °C for 3 h. For the preparation of magnetic carbonaceous particles with a richer carboxyl content, 10 v/v% (1.5 mL) acrylic acid was added into the 0.5 M glucose solution for hydrothermal carbonization.[33] A brownish suspension was obtained after hydrothermal carbonization. The suspended particles were collected using a magnet and washed with 70% ethanol (250 mL) for 3 times followed by DI water (250 mL). The particles collected by a magnet were designated as MH@C and MH@C−Ac for carbonaceous passivation without and with acrylic acid addition, respectively.

2.4. Analysis and Characterization of MNPs. The surface charge of the particle was determined using a zeta potential analyzer (Zetasizer 2000, Malvern Instrument, Malvern, UK). MNPs of 50 mg were dispersed in 15 mL of a 0.01 M NaCl solution, pH adjusted between 2 and 12 using 0.1 N HCl or NaOH solutions. The Brønsted acid sites in the MNPs were determined by the neutralization titration method. Briefly, a 20 mL solution of 1 M NaCl and 40 mg of MNPs were added. The mixture was sonicated for 20 min and shaken for 24 h at room temperature. After centrifugation, the supernatant was titrated by 0.01 N NaOH and phenolphthalein was used as an indicator. The amine content on the MNP surface was determined using a ninhydrin test.[34] Transmission electron microscopy (TEM) images were taken using a Hitachi H-800 transmission electron microscope (Japan). TGA (Perkin-Elmer, Diamond TG/DTA) was carried out from ambient temperature to 700 °C under nitrogen atmosphere at a heating rate of 10 °C/min. The carbon content in the MNPs was estimated by the percentage of weight loss from the corresponding TGA curves. Fourier transform infrared spectrometry (Biorad, Digilab FTS-3500) was used for the identification of the functional groups on the particle surface. The Ni^{2+} ion concentration was measured by an inductively coupled plasma atomic emission spectrophotometer (ICP-AES JY2000 2, HORIBA Jobin Yvon).

2.5. Production of 6×His Tagged GFP and HA Lyase. The GFP expression plasmid constructed based on pET 30b was transformed into *E. coli* BL21(DE3) for GFP expression. A single colony on the selection agar was picked and inoculated into 5 mL of Luria−Bertani (LB) medium containing 100 μg/mL ampicillin. The culture was shaken overnight at 37 °C at 200 rpm and used as inoculums. The inoculated LB broth (amp+) was grown at 37 °C with vigorous shaking and isopropyl-β-D-thiogalacto-pyranoside (IPTG) was added to a final concentration of 1 mM when optical density (OD) at 600 nm reached 0.8. The cells were harvested after 12 h by centrifugation at 8000 rpm for 10 min at 4 °C. GFP was released from the *E. coli* cell pellet by sonication in 50 mM, pH 7.5 phosphate buffer containing 0.5 M NaCl. After centrifugation at 9000 rpm for 20 min at 4 °C, the supernatant obtained was used as crude extract for GFP isolation.

For HA lyase production, the recombinant strain *E. coli* BL21 (DE3)/pET30b-hylp was grown overnight at 37 °C in LB medium containing 50 g/mL kanamycin. The cultures were diluted (1:100) by fresh LB kanamycin media and incubated at 37 °C with 200 rpm shaking. HA lyase expression was induced by adding IPTG to give a final concentration of 1 mM when the culture OD at 600 nm reached 0.8. After 3 h induction, the cells were harvested by centrifugation at 8000 rpm for 20 min at 4 °C. Then, the cell pellets were washed twice using 0.1 M phosphate buffer, pH 7.4, and resuspended in 4 mL (100 mL of culture) of 20 mM, pH 7.4 phosphate buffer containing 500 mM NaCl, 20 mM imidazole, 1 mg/mL lysosyme, 0.1% Triton X-100, and 1 mM PMSF and kept in ice for 30 min before sonication. The HA lyase released from the sonicated *E. coli* cell pellet was centrifuged at 8000 rpm for 20 min at 4 °C. The obtained supernatant was used as crude extract for HA lyase isolation.

2.6. Affinity Isolation of GFP and HA Lyase by MNPs with Carbonaceous Shell. MH@C or MH@C−Ac (0.1 g) was charged with 1.5 mL of 0.5 M $NiSO_4$ solution and incubated at 25 °C for 24 h. The Ni^{2+} ion concentration in the supernatant was immediately determined by ICP-AES. The decreased Ni^{2+} ion concentration was considered as the amount captured by MNPs. The MNPs was washed thoroughly with DI water followed by 6 mL of washing buffer (50 mM, pH 7, phosphate buffer containing 0.1 M NaCl). All the solid−liquid separation was carried out using a magnet. The crude extract of GFP or HA lyase of 200 μL along with 800 μL of washing buffer were well-mixed with the washed MNPs for 1 h at 4 °C. The proteins remaining in the supernatant were considered as the unbound proteins. After washing the MNPs with 4 mL of washing buffer, 200 μL of eluting buffer (10 mM, pH 7, phosphate buffer containing 250 mM imidazole containing 0.1 M NaCl) was added to elute the captured proteins by incubating at 4 °C for 1 h under mild shaking.

2.7. Analysis. The protein concentration was determined by Bradford protein assay using bovine serum albumin (BSA) as a standard.[35] Sodium dodecyl sulfate-polyacrylamide gel electrophoresis (SDS-PAGE) analysis was carried out in a 12% polyacrylamide gel.[36] The HA lyase activity was determined as the release rate of *N*-acetyl-glucosamine (NAG) equivalents measured by the modified Elson−Morgan method.[37] The 37.5 μL eluted protein solution was incubated with 37.5 μL of 2 mg m/L HA solution prepared in pH 6, 0.1 M phosphate buffer supplemented with 0.1 M NaCl and 75 μL of 0.1 mg/mL BSA, at 37 °C. The amount of the HA lyase that releases 1 μmol of product per minute at 37 °C was considered as one enzyme unit. The recovery yield of HA lyase is defined as the ratio of amount of HA lyase activity in the eluted solution to that in the crude extract.

3. RESULTS AND DISCUSSION

3.1. Magnetic Nanoparticles Preparation and Characterization. The original dark-orange solution prepared by dissolving

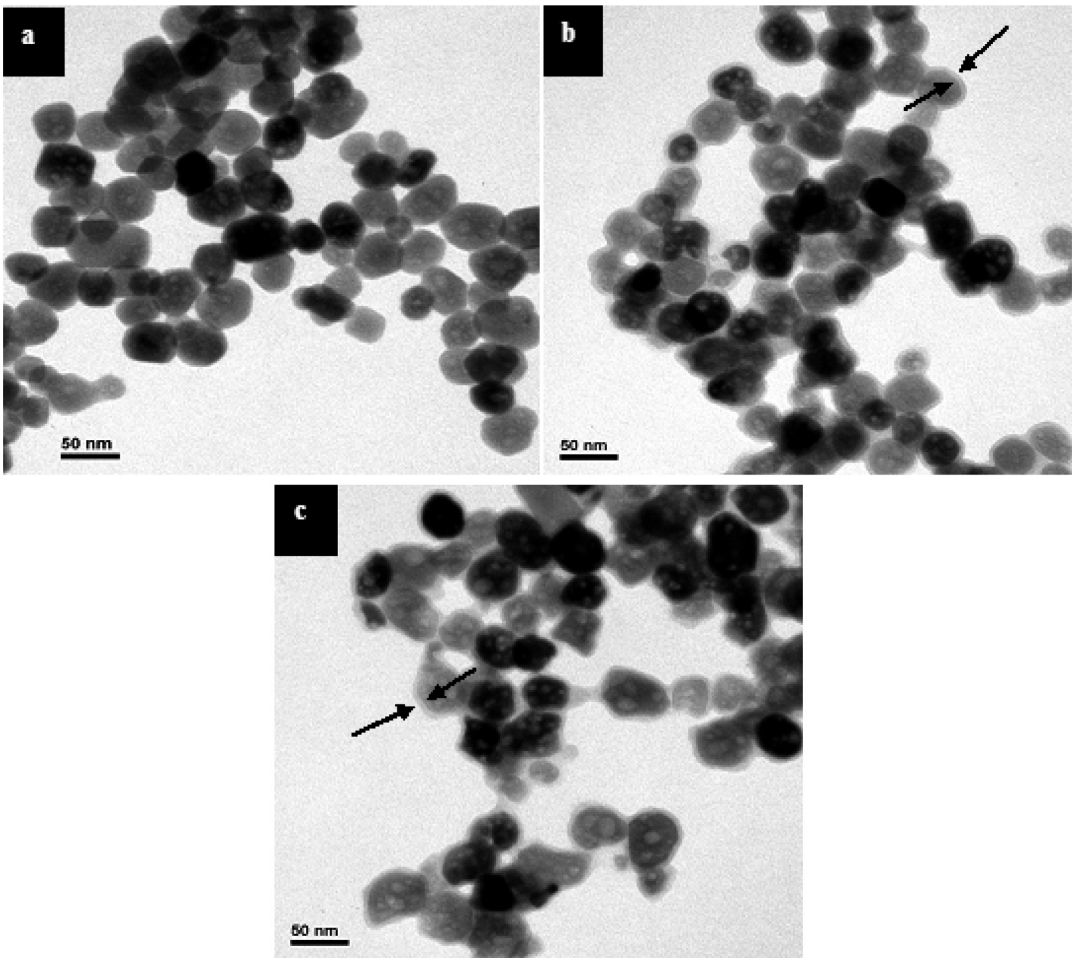

Figure 1. TEM images of (a) surface amine-functionalized MNPs (MH), (b) carbonaceous material passivated MH (MH@C), and (c) carbonaceous passivation in the presence of 10 w/v% acrylic acid (MH@C−Ac).

$FeCl_3$ and 1,6-hexanediamine in ethylene glycol turned into a stable black suspension after heating at 198 °C for 6 h. The suspension could be easily clarified by applying an external magnetic field. The black precipitate collected was considered as the surface amine-functionalized MNPs (MH). A brownish suspension was obtained after hydrothermal carbonization of the blackish MH suspended glucose solution. The brownish color resulted from the degradation products of glucose (furfural, hydroxymethylfurfural, etc.) and their dehydration polymerization products.[38] These carbonaceous materials are expected to be passivated on the surface of suspended MH during the carbonization reaction. Therefore, the suspended particles that could be collected by a magnet were considered as our desired product MH@C. A small fraction of precipitate, which did not respond to the magnetic field, was also observed, which should be the carbonaceous materials that did not graft onto the surface of MH.

As observed by TEM (Figure 1a), the MH before carbonization treatment is round shaped with a diameter in the range of 30 nm. Out of our expectation, the hydrothermal treatment in glucose solution seems slightly to reduce the size of MH (Figure 1b). It is known that the high pressure water is quite acidic[39−41] and an appreciable amount of acidic byproduct will be generated in the hydrothermal carbonization reaction.[38] The final pH of MH@C suspension prepared from hydrothermal carbonization of glucose was also measured to be 3.3. Therefore, the observed slight size reduction of MH@C is presumably due to the erosion of MH that occurred in the acidic hydrothermal environment before carbonaceous shell was passivated on. The thin carbonaceous layer of MH@C is hydrophilic and has a distribution of −OH and −COOH groups. When acrylic acid was present in the carbonization reaction to enhance the carboxylic content in the carbonaceous shell,[22] the size of MH@C−Ac (Figure 1c) was not much affected. A thin shell about a few nanometer thicknesses at the periphery of MH@C and MH@C−Ac could be observed (Figure 1b,c). As shown in the FTIR spectra (Figure 2), an apparent amine band (1645 cm^{-1}) was noticed on the surface of MH and an Fe−O band (598 cm^{-1}) was observed for all the MNPs. The adsorption bands of C═C double bonds (1620 cm^{-1} and 1400 cm^{-1}), C−OH stretching, and OH bending vibrations (1000−1300 cm^{-1}) could only be observed for MH@C. The strong adsorption intensity for C═O (1700 cm^{-1}) corresponding to the carboxylic group was only observed for MH@C−Ac. This indicates that a higher degree of carboxylic group modification of MH was achieved by adding acrylic acid in the carbonization reaction. The carboxylic acid content could be increased 50% from 0.190 mmol/g to 0.285 mmol/g when acrylic acid was added. This is probably because the acrylic acid as a functional monomer participates in the polymerization process of the decomposed glucose products to form the carbonaceous shell on MH@C−Ac.

The existence of passivated carbonaceous shell and its homogeneity on MH@C and MH@C−Ac were also verified using the ninhydrin test. The principle of this test is that once the surface amine group reacts with ninhydrin it will leave the surface to form a purple colored molecule in solution. As shown in Figure 3, the solution of naked MH shows the typical purple color of the ninhydrin test (Figure 3a) which indicates the presence of an amine-functionalized surface. In contrast, only the background color of pale yellow was observed for MH@C and MH@C−Ac (Figure 3b,c). This indicates that the MH was well passivated by the carbonaceous shell on both MH@C and MH@C−Ac so that ninhydrin molecules cannot penetrate through to react with the amine groups on the surface of MH. Probably, the amine-functionalized surface of the well-dispersed MH provides the grafting sites for the degraded glucose products (carbonaceous precursors) to polymerize into carbonaceous materials around MH. The magnetic core of MH@C is still maintained as magnetite (Fe_3O_4) after hydrothermal carbonization, as indicated by its crystalline structure analysis, but its saturation magnetization decreases slightly as shown in our previous work[14] and in the Supporting Information (Figure S1).

The successful passivation of carbonaceous materials on MH could also be confirmed by TGA analysis. As shown in Figure 4, up to 700 °C less than 9% weight loss was detected for MH. On the other hand, a very sharp weight loss was observed for MH@C and MH@C−Ac at 650 °C, it was due to degradation and aromatization of the structural network of carbonaceous layers[42] (Supporting Information, Figure S2). Although the weight loss behaviors were quite different during the heating under N_2, the final weight loss leveled off to 50% for both MH@C and MH@C−Ac at 700 °C. This indicates that approximately 50% of the as-prepared MH@C and MH@C−Ac is carbonaceous materials. MH@C−Ac demonstrated a heavier weight loss than MH@C in the range of 350 to 650 °C, and an apparent loss could be observed around 430 °C. This shows that the carbonaceous material passivated on MH became less thermally stable when acrylic acid was added as a functional monomer to enhance the carboxylate content. The similar TGA result has also been reported on carbonaceous sphere formation in hydrothermal carbonization in the presence of acrylic acid.[21] Probably, the carboxylic acid groups of acrylic acids participating in the polymerization of degraded glucose prevent a stronger structural network formation on the surface of MH.

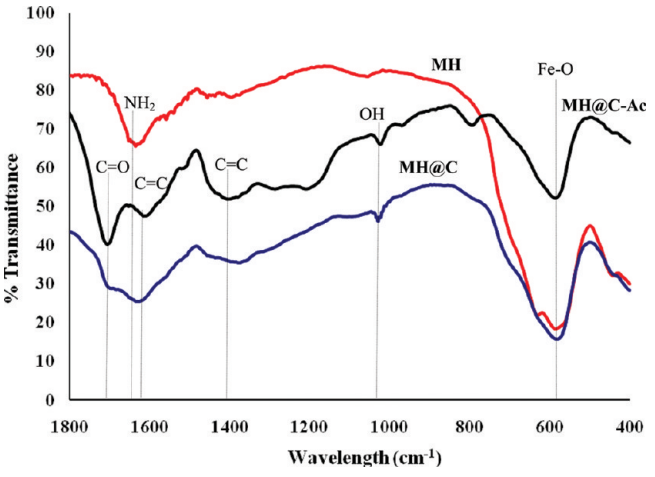

Figure 2. FTIR spectra of amine-functionalized MNPs (MH) and carbonaceous material passivated MNPs (MH@C and MH@C−Ac).

The surface charge of MH, MH@C, and MH@C−Ac particles were studied by measuring their zeta potentials at pH ranging from 2 to 12. As shown in Figure 5, the zeta potentials decrease with pH, and because of the presence of amine groups on the surface of MH, the MH particle possesses the point of zero charge (PZC) at pH around 6.5. The PZC decreases to pH around 2.5 after carbonization treatment which indicates the presence of an appreciable amount of an acidic carbonaceous layer on the surface of MH@C and MH@C−Ac. In comparison with that of MH@C, the surface charge of MH@C−Ac is more negative. This indicates the surface of MH@C−Ac is richer in carboxylic groups resulting from the added acrylic acid.

3.2. 6×His Tagged Recombinant Proteins Isolation. The carboxylate-rich carbonaceous layer on the magnetic particles was employed for immobilizing the Ni^{2+} ion via divalent or trivalent coordination interaction with carboxylate groups. The immobilized Ni^{2+} will act as a ligand to participate in the specific binding with the His tag of recombinant proteins. The schematic diagram for isolating the recombinant 6×His tagged protein by MH@C and MH@C−Ac is shown in Scheme 1. Before being employed for protein isolation, the particles were charged with Ni^{2+} ion by incubating in Ni^{2+} solution for 24 h. The amount of Ni^{2+} disappearing from the supernatant was considered as being adsorbed in the carbonaceous shell of MH@C and MH@C−Ac. Approximately, 61.12 mg/g and 85.91 mg/g of Ni^{2+} ions were adsorbed by MH@C and MH@C−Ac, respectively. After thorough washing with buffer solution (50 mM, pH 7 phosphate

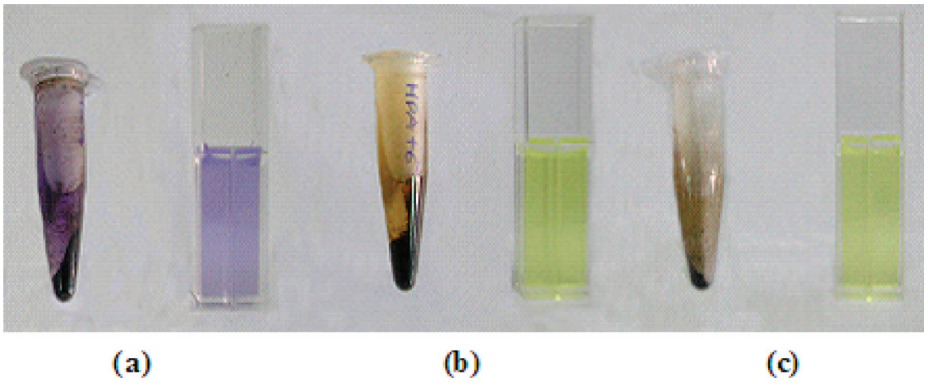

Figure 3. Ninhydrin test for MNP surface amine assay: (a) amine-functionalized MNPs (MH), (b) carbonaceous material passivated MH (MH@C), (c) carbonaceous passivated MH prepared in the presence of 10 w/v% acrylic acid (MH@C−Ac).

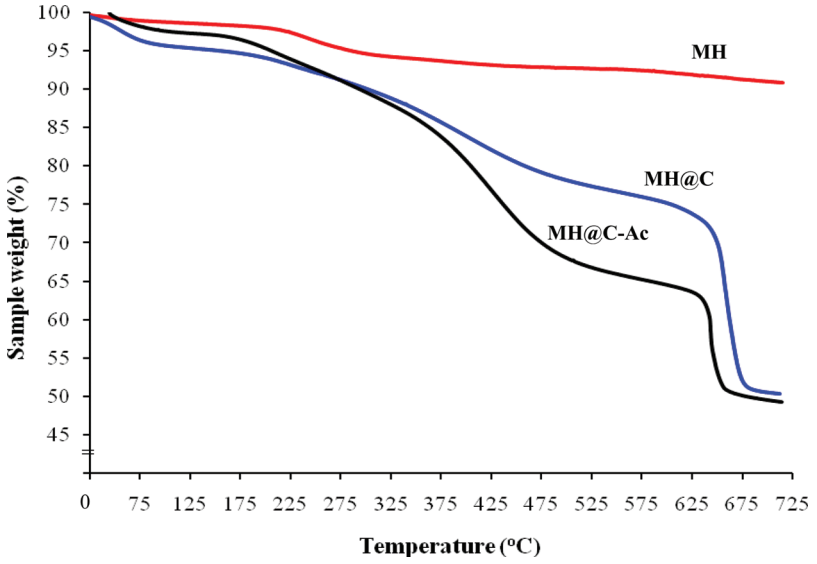

Figure 4. TGA curve of amine-functionalized MNPs (MH), carbonaceous material passivated MH (MH@C), and carbonaceous passivated MH prepared in the presence of 10 w/v% acrylic acid (MH@C−Ac).

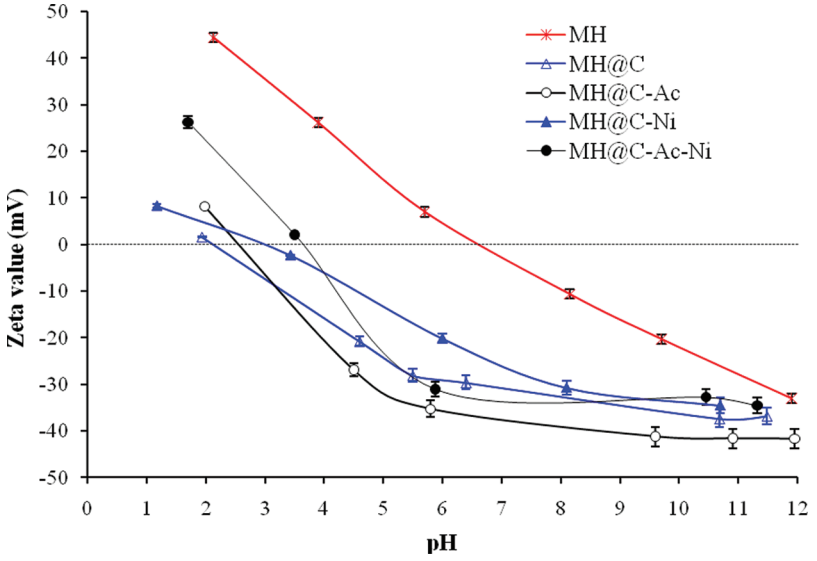

Figure 5. pH effect on zeta potentials of surface amine-functionalized MNPs (MH), carbonaceous material passivated MH (MH@C and MH@C−Ac), and Ni^{2+} ion complexed MH@C−Ni and MH@C−Ac−Ni.

buffer) to remove the leachable Ni^{2+} ions such as those interacted with a single carboxylate group, the particles were employed for further characterization and protein purification. The strong binding of Ni^{2+} ion to the carboxylic groups was also reflected by the apparent increase of zeta potential of the thoroughly washed Ni^{2+} charged MH@C and MH@C−Ac (Figure 5). A larger increase of zeta potential was observed for the carboxylate-rich MH@C−Ac. Evidently, the increase of zeta potential resulted from the neutralization of the negatively charged carboxylate groups with Ni^{2+} ion. The carbon coating is required in this experiment not only because it provides the rich carboxylate groups for immobilizing Ni^{2+} ion to specifically capture the His-tagged proteins but also because, after several repeated use of the nanoparticles, an acidic solution was required to be used for the regeneration of the particles by removing the foulants from the surface. At this regeneration condition, the magnetite core was well protected by the carbon coating.

As shown in Table 1, no appreciable protein was adsorbed by MH@C without charging Ni^{2+} in the case of crude GFP extract. In contrast, 6.23 mg of protein was adsorbed by one gram of uncharged MH@C−Ac. Evidently, the rich carboxylic groups on the surface of MH@C−Ac will nonspecifically interact with GFP protein.[6] When Ni^{2+} ion was immobilized on the particle, the protein adsorption capacity increased 6-fold from 0.026 to 1.316 mg/g for MH@C. However, only 1.5-fold (9.41 mg/g) enhancement was obtained for MH@C−Ac. In other words, the higher amount of Ni^{2+} adsorbed on MH@C−Ac did not give a higher enhancement on GFP adsorption. Only the Ni^{2+} ions complexed on the surface of the carbonaceous layer may have the chance to interact with the His-tagged protein (Scheme 1). The SDS-PAGE (Figure 6)

Scheme 1. Schematic Diagram for the Preparation of Carbonaceous Material Passivated Magnetic Nanoparticles and Its Application for Isolating Recombinant 6×His-Tagged Protein

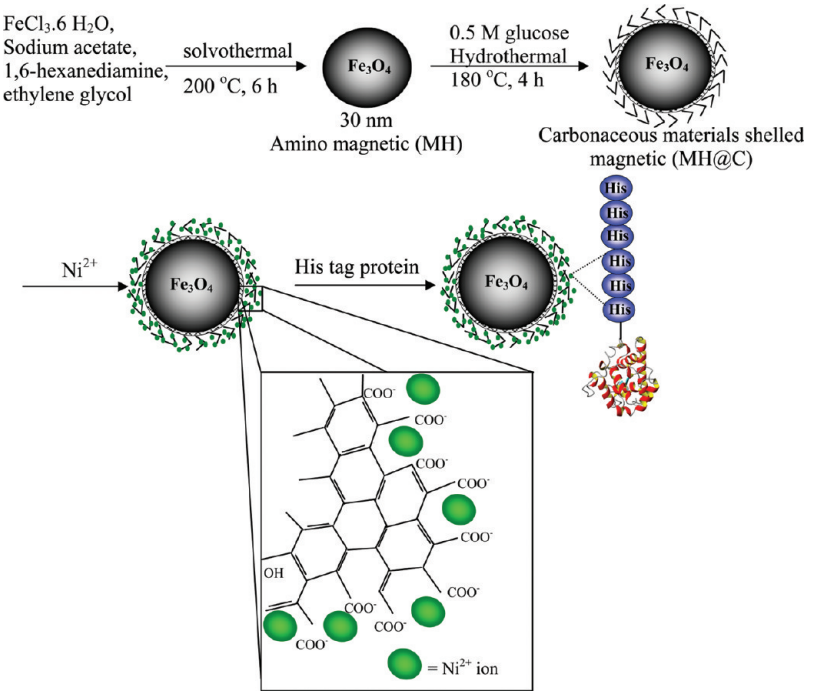

Table 1. Amount of GFP Captured by Carbonaceous Material Passivated MNPs

magnetic adsorbents	MH@C	MH@C−Ac	MH@C−Ni	MH@C−Ac−Ni
protein binding capacity (mg/g)	0.026	6.229	1.316	9.410

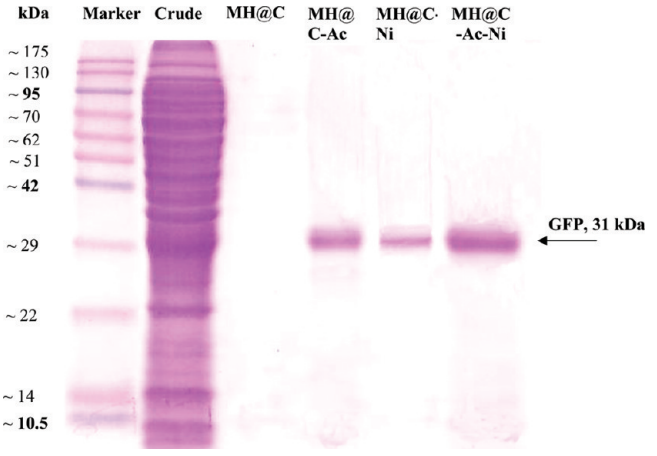

Figure 6. SDS-PAGE analysis of GFP isolation by various carbonaceous material passivated magnetic nanoparticles.

analysis of the isolated GFP (31 kDa) can further confirm that the higher binding capacity of MH@C−Ac as compared with MH@C because an apparent GFP band could be observed in the use of MH@C−Ac. The existence of this quite pure GFP band is probably

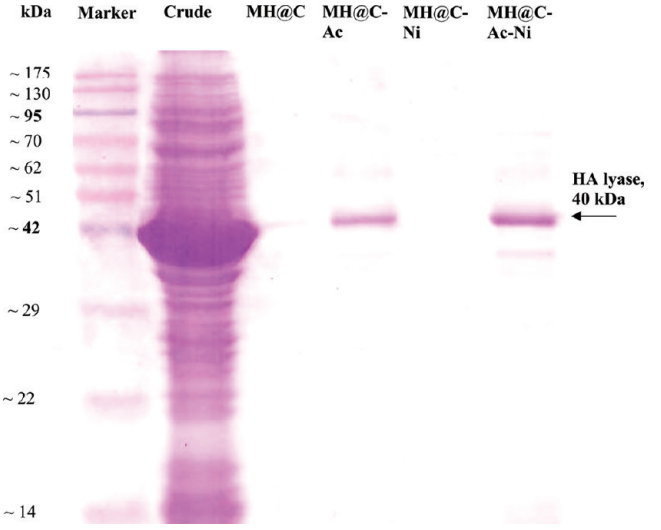

Figure 7. SDS-PAGE analysis of HA lyase isolation by various carbonaceous material passivated magnetic nanoparticles.

because the overexpressed GFP is the major protein in the crude extract of recombinant *E. coli* and the rich carboxylate groups on the surface of MH@C−Ac will have a much higher chance to interact with the major GFP rather than other minor contaminant proteins. Besides, the total protein concentration loaded for SDS-PAGE analysis is so low that only the major protein can be clearly observed. When Ni^{2+}charged particles were employed, a significantly thicker GFP band was observed as compared with its counterpart. These indicate that the Ni^{2+} immobilized on the surface of a carbonaceous layer can specifically capture the 6×His-tagged GFP and with GFP binding capacity of MH@C−Ac higher than that of MH@C.

Table 2. HA Lyase Purification Table Using Various Carbonaceous Material Passivated MNPs

sample	protein eluted (mg)	capacity (mg/g)	activity (U)	specific activity (U/mg)	yield (%)	purification factor
crude extract	1.844		0.604	0.328	100	1.00
MH@C	not detectable					
MH@C−Ac	0.173	1.729	0.077	0.445	13	1.358
MH@C−Ni	0.007	0.069				
MH@C−Ac−Ni	0.230	2.314	0.304	1.321	50	4.033

For the isolation of 6×His tagged HA lyase, approximately 2.31 mg/g protein was adsorbed by MH@C−Ac−Ni as shown in Table 2. It was about 1.3-fold higher than that obtained for MH@C−Ac (1.73 mg/g), but most of proteins captured by MH@C−Ac only showed appreciable HA lyase activity (0.077 U) while those captured by MH@C−Ac−Ni had much higher activity (0.304 U). The recovery yield of HA lyase increased significantly to 50% and with a 4-fold increase of purification factor when MH@C−Ac−Ni was employed. This again shows the immobilized Ni^{2+} facilitates the isolation of the 6×His tagged HA lyase. As shown in SDS-PAGE (Figure 7), only one band located around 40 kDa, which corresponds to the molecular weight of recombinant HA lyase, was observed for both MH@C−Ac and MH@C−Ac−Ni but with a thicker band for MH@C−Ac−Ni. However, no appreciable amount of protein could be detected in the solution eluted from MH@C and MH@C−Ni. Probably, His-tag domain of the recombinant HA lyase is not easily accessible to the Ni^{2+} immobilized on MH@C. On the other hand, in MH@C−Ac (which is prepared with additional acrylic acid), the carboxylate groups may exist near the outer surface of the layer which can be easily reached by the His-tagged proteins. Furthermore, HA lyase is a cationic protein with pI about 8.75 and known to have interaction with carboxylic acid or hydroxyl groups on the hydrophilic substrates.[33,43] The richer content of carboxylate groups on the surface of MH@C−Ac enhances its electrostatic interaction with the cationic HA lyase. The Ni^{2+} immobilized on MH@C−Ac−Ni can further promote the metal affinity interaction with the 6×His tagged on HA lyase which is electrostatically attracted to the surface of particles. As a consequence, an apparent increase of HA lyase adsorption was obtained for the Ni^{2+} immobilized MH@C−Ac as shown in Table 2 and Figure 7.

Since the preparation of carbonaceous material passivated magnetite nanoparticles is a straightforward process, different batches of preparation did not give much difference in the amount of Ni^{2+} ion adsorbed and specific affinity toward the same recombinant protein. The protein binding capacity of the as-prepared particles is protein dependent. Different His-tagged recombinant proteins will strongly affect the purification results because of the intrinsic structures of the proteins. The protein binding capacity was compared with GE Fast flow Ni-Sepharose gel as shown in Table T1 in Supporting Information. The binding capacity of MH@C−Ac−Ni toward GFP is only about 10% less than that of GE Ni-Sepharose gel. The higher binding capacity of gel-type Ni-Sepharose is mainly the result from its porous structure which provides a higher specific area for the immobilization of Ni^{2+} ions. However, the porous structure may exclude larger size proteins from approaching the immobilized Ni^{2+} ions and prolong the time required to reach saturation binding. On the other hand, the as-prepared MH@C−Ac−Ni has a size (~50 nm) much smaller than the gel-type Ni-Sepharose and the protein binding only occurs in the thin carbonaceous layer. The protein binding kinetic should be much faster than the commercial Ni-Sepharose gel. Therefore, the quicker binding, washing, and elution cycle can be repeated many times to compensate the lower binding capacity of MH@C−Ac−Ni so that the overall productivity for isolation of His-tagged recombinant proteins will be comparable with those commercial gel-type porous beads.

4. CONCLUSIONS

Magnetic nanoparticle with a thin carbonaceous shell can be easily prepared via a two-step thermal synthesis in solution phase at temperature near 200 °C. Carbonaceous shell could be favorably passivated on the surface amine-functionalized MNPs when hydrothermally carbonized in 0.5 M glucose solution with and without the presence of acrylic acid. The point of zero charge (PZC) of particles decreased after carbonaceous shell passivation because of its rich carboxylic acid content. The carboxylate-rich carbonaceous shell has a high capability to complex with Ni^{2+} ions, and the superparamagnetic property of MNPs@C can facilitate the isolation of 6×His tagged proteins. In addition, the small size (~50 nm) and nearly nonporous structure of the as-prepared immobilized metal MNP will shorten the binding time when compared with the commercial gel-type counterparts. Furthermore, the good physical properties of magnetic, chemical stability and a rich-carboxylic acid functionalized surface will make the carbonaceous magnetic nanoparticles have broader potential applications such as in the fields of catalysis, drug delivery, and enzyme immobilization.

■ ASSOCIATED CONTENT

Supporting Information. Magnetization curves of MH and MH@C; TGA-derivative curve of MH, MH@C, and MH@C−Ac; and comparison of GFP and HA lyase binding capacity between carbonaceous material passivated MNPs and GE Sepharose gel. This material is available free of charge via the Internet at http://pubs.acs.org.

■ AUTHOR INFORMATION

Corresponding Author

*Fax: +886 2 2737 6629. Tel: +886 2 2737 6644. E-mail: cklee@mail.ntust.edu.tw.

■ ACKNOWLEDGMENT

The authors are grateful for the financial support from Directorate General of Higher Education, Ministry of National Education, Republic of Indonesia, which provides a scholarship for I.F.N. (academic staff of Lambung Mangkurat University, Indonesia) during her study in National Taiwan University of Science and Technology (NTUST) Taiwan.

REFERENCES

(1) Pan, C.; Hu, B.; Li, W.; Sun, Y.; Ye, H.; Zeng, X. *J. Mol. Catal. B: Enzym.* **2009**, *61*, 208–215.
(2) Frenzel, A.; Bergemann, C.; Köhl, G.; Reinard, T. *J. Chromatogr., B* **2003**, *793*, 325–329.
(3) Girault, S.; Chassaing, G.; Blais, J. C.; Brunot, A.; Bolbach, G. *Anal. Chem.* **1996**, *68*, 2122–2126.
(4) Ma, Z.; Liu, H. *China Particuology* **2007**, *5*, 1–10.
(5) Nishio, K.; Masaike, Y.; Ikeda, M.; Narimatsu, H.; Gokon, N.; Tsubouchi, S.; Hatakeyama, M.; Sakamoto, S.; Hanyu, N.; Sandhu, A.; Kawaguchi, H.; Abe, M.; Handa, H. *Colloids Surf., B* **2008**, *64*, 162–169.
(6) Peng, Z. G.; Hidajat, K.; Uddin, M. S. *J. Colloid Interface Sci.* **2004**, *271*, 277–283.
(7) Obata, K.; Segawa, O.; Yakabe, M.; Ishida, Y.; Kuroita, T.; Ikeda, K.; Kawakami, B.; Kawamura, Y.; Yohda, M.; Matsunaga, T.; Tajima, H. *J. Biosci. Bioeng.* **2001**, *91*, 500–503.
(8) Wei, X.-W.; Zhu, G.-X.; Xia, C. J.; Ye, Y. *Nanotechnology* **2006**, *17*, 4307–4311.
(9) Li, U.-y.; Jiang, Y.-e.; Huang, K.-l.; Ding, P.; Chen, J. *J. Alloys Compd.* **2008**, *466*, 451–456.
(10) Girginova, P. I.; Daniel-da-Silva, A. L.; Lopes, C. B.; Figueira, P.; Otero, M.; Amaral, V. S.; Pereira, E.; Trindade, T. *J. Colloid Interface Sci.* **2010**, *345*, 234–240.
(11) Deng, Y.-H.; Wang, C.-C.; Hu, J.-H.; Yang, W.-L.; Fu, S.-K. *Colloids Surf., A* **2005**, *262*, 87–93.
(12) Ikeda, S.; Tachi, K.; Ng, Y. H.; Ikoma, Y.; Sakata, T.; Muri, H.; Harada, T.; Matsumura, M. *Chem. Mater.* **2007**, *19*, 4335–4340.
(13) Zhang, Z.; Duan, H.; Li, S.; Lin, Y. *Langmuir* **2009**, *26*, 6676–6680.
(14) Nata, I. F.; Salim, G. W.; Lee, C.-K. *J. Hazard. Mater.* **2010**, *183*, 853–858.
(15) Heebøll-Nielsen, A.; Choe, W. S.; Middelberg, A. P. J.; Thomas, O. R. T. *Biotechnol. Prog.* **2003**, *19*, 887–898.
(16) O'Brien, S. M.; Sloane, R. P.; Thomas, O. R. T.; Dunnill, P. *J. Biotechnol.* **1997**, *54*, 53–67.
(17) O'Brien, S. M.; Thomas, O. R. T.; Dunnill, P. *J. Biotechnol.* **1996**, *50*, 13–25.
(18) Campo, A. d.; Sen, T.; Lellouche, J.-P.; Bruce, I. J. *J. Magn. Magn. Mater.* **2005**, *293*, 33–40.
(19) Heebøll-Nielsen, A.; Justesen, S. F. L.; Thomas, O. R. T. *J. Biotechnol.* **2004**, *113*, 247–262.
(20) Nata, I. F.; Lee, C. K. *Green Chem.* **2010**, *12*, 1454–1459.
(21) Demir-Cakan, R.; Baccile, N.; Antonietti, M.; Titirici, M. M. *Chem. Mater.* **2009**, *21*, 484–490.
(22) Yi, J. X.; Weinberg, G.; Liu, X.; Timpe, O.; Schlögl, R.; Su, D. S. *Adv. Funct. Mater.* **2008**, *18*, 3613–3619.
(23) Zhuang, R.; Zhang, Y.; Zhang, R.; Song, C.; Yang, K.; Yang, A.; Jin, B. *Protein Expression Purif.* **2008**, *59*, 138–143.
(24) Chiang, C. L.; Chen, C. Y.; Chang, L. W. *J. Chromatogr., B* **2008**, *864*, 116–122.
(25) Penna, T.; Ishii, M.; Junior, A.; Nascimento, L.; de Souza, L.; Cholewa, O. *Appl. Biochem. Biotechnol.* **2004**, *114*, 453–468.
(26) El-Safory, N. S.; Lee, C.-K. *Carbohydr. Polym.* **2010**, *82*, 1116–1123.
(27) Yang, P.-F.; Lee, C.-K. *Biochem. Eng. J.* **2007**, *37*, 108–115.
(28) Stern, R.; Jedrzejas, M. J. *Chem. Rev.* **2006**, *106*, 818–839.
(29) Tawada, A.; Masa, T.; Oonuki, Y.; Watanabe, A.; Matsuzaki, Y.; Asari, A. *Glycobiology* **2002**, *12*, 421–426.
(30) Baker, J. R.; Dong, S.; Pritchard, D. G. *Biochem. J.* **2002**, *365*, 317–322.
(31) Ingham, E.; Holland, K. T.; Gowland, G.; Cunliffe, W. J. *J. Gen. Microbiol.* **1979**, *115*, 411–418.
(32) Wang, L.; Bao, J.; Wang, L.; Zhang, F.; Li, Y. *Chem.—Eur. J.* **2006**, *12*, 6341–6347.
(33) Suh, K. Y.; Yang, J. M.; Khademhosseini, A.; Berry, D.; Tran, T.-N. T.; Park, H.; Langer, R. *J. Biomed. Mater. Res., Part B: Appl. Biomater.* **2004**, *72B*, 292–298.
(34) Rosen, H. *Arch. Biochem. Biophys.* **1957**, *67*, 10–15.
(35) Bradford, M. M. *Anal. Biochem.* **1976**, *72*, 248–254.
(36) Hames, B. D. *One-dimensional polyacrylamide gel electrophoresis*; IRL Press: Oxford, England, 1986, 1−147.
(37) Reissig, J. L.; Strominger, J. L.; LEL, L. F. *J. Biol. Chem.* **1955**, *217*, 959–966.
(38) Sevilla, M.; Fuertes, A. B. *Chem.—Eur. J.* **2009**, *15*, 4195–4203.
(39) Brunner, G. *J. Supercrit. Fluids* **2009**, *47*, 373–381.
(40) Sue, K.; Uchida, M.; Usami, T.; Adschiri, T.; Arai, K. *J. Supercrit. Fluids* **2004**, *28*, 287–296.
(41) Kritzer, P. *J. Supercrit. Fluids* **2004**, *29*, 1–29.
(42) Zhao, L.; Bacsik, Z.; Hedin, N.; Wei, W.; Sun, Y.; Antonietti, M.; Titirici, M.-M. *ChemSusChem* **2010**, *3*, 840–845.
(43) Furth, G.; Knierim, R.; Buss, V.; Mayer, C. *Int. J. Biol. Macromol.* **2008**, *42*, 33–40.